J. Indian Inst. Sci., May–June 1989, **69**, 193–211.

Sliding-mode control of power converters*

V. RAMANARAYANAN†, ASIF SABANOVIC†† AND SLOBODAN CUK
Power Electronics Group, California Institute of Technology, Pasadena, CA91125, USA.

Received on May 10, 1988; Revised on October 18, 1988.

Abstract

The theory of variable structure systems [VSS] presents an elegant method to describe dc-to-dc power converters. An analysis method of control systems with sliding mode—the equivalent control method—provides a simple analysis tool to obtain equivalent continuous system representation of such time-varying systems. In this paper power converters are explored in the light of these concepts to arrive at large- and small-signal models. Experimental results are then presented verifying these concepts.

Keywords: Power converters, switched-mode power supply, sliding-mode control.

1. Introduction

The theory of VSS and sliding-mode control has been extensively explored theoretically[1]. Recently application of this theory to dc-to-dc converters has been reported[2]. It introduces the development of a sliding-mode controller for a dc-to-dc chopper converter, with results for a 500W converter highlighting the robustness of such converters in the presence of parameter uncertainties.

In the past the method of state-space averaging has been widely used to analyse dc-to-dc converters[3]. In the state-space averaging method, the linear circuit models and the resultant state-space equations are identified for each of the possible switch positions of the converter over a switching period. These state-space equations are then averaged over a swithching period to arrive at the low-frequency equivalent model of the converter. The low-frequency model thus obtained may be linearised in order to apply linear control theory to design feedback compensators that achieve the design requirements. In essence the state-space averaging provides a method of low-frequency characterisation of converters so that frequency domain design techniques may be applied to the control problem. The number of poles of the system is equal to the number of storage elements in the converter, which

*This work was supported in part by the General Dynamics Corporation, Fort Worth, Texas and by Caltech's Advanced Technologies, sponsored by Aerojet General, General Motors, GTE, and TRW.
†Presently with the Department of Electrical Engineering, Indian Institute of Science, Bangalore, 560012, India.
††Presently with Energoinvest – IRCA, Sarajevo, Yugoslavia.

may be several; add to these possibly one or more right half-plane [RHP] zeroes, and the design of a satisfactory controller can be exasperating. Besides since one is working with the small-signal model nothing can be guaranteed about the large-signal behaviour or the stability of the system.

As opposed to the above, the theory of VSS and sliding-mode control are time-domain techniques. The theory of VSS may be used to characterise the system for both small- and large-signal conditions. Sliding-mode control uses multiple state feedback, and sets up directly the desired closed-loop response in the time domain. Most important of all, the response is, for all practical purposes, independent of the system parameters.

In the following sections, a brief introduction to VSS is given. From the general theory of sliding-mode control, the concept of equivalent control is explained and demonstrated for the case of constant frequency-duty-ratio-controlled converters.

The equivalent control method of analysing switching converters as VSS, and the state-space averaging method of analysis of switching converters follows different mathematical formalism to arrive at essentially the same low-frequency models for the converters. In the past, linearisation of the state-space averaged model has led to the application of classical control methods such as loop-shaping to the control problem of the dc-to-dc converters. In contrast to this, the sliding-mode control tackles the control problem directly in the time domain.

For dc-to-dc converters which are largely second-order systems, the concept of sliding-mode control may be brought out much more strikingly by consideration of the phase plane. In this paper, control of dc-to-dc buck converter is demonstrated through the phase-plane representation. Such a presentation helps one better appreciate the strengths of sliding-mode control, and is intuitively more satisfying.

It will be noted from the example that application of sliding-mode control requires all the controllable states (*i.e.* the output and its derivatives) of the system to be continuous and accessible. For the boost and buck-boost converters the controllable states are not all continuous. One then takes a different approach by considering inductor-current control[3]. Essentially inductor-current control is accomplished by any one of a number of methods of switching strategies in order to maintain the current through the inductor at a desired level. Since the inductor current and in turn the stored energy in the inductor remains constant under such a control, the inductor ceases to be a dynamic element of the converter. All three topologies of dc-to-dc converters in that case are of reduced order and equally amenable to the application of sliding-mode control. Application of equivalent control method provides an equivalent continuous system model for free running as well as constant frequency current-controlled converters. The transfer function description may also be readily obtained. In addition, an alternative method of describing switching converters in terms of the power handled by the converter emerges out of this exercise, and such a description allows an indirect method of setting up a satisfactory control strategy for the voltage control of boost and buck-boost converters.

Practical realisation of the control strategy and experimental results verifying the control method are then presented.

2. Variable structure systems [VSS]

VSS are characterised by a time-variant topology, and as a result the control action is discontinuous and the plant nonlinear. In switched-mode converters the control action is discontinuous and they all fall into the category of VSS.

Figure 1 shows the three basic switching converter topologies and their inductor current waveforms. The switch position defines the control input u as shown in fig. 1. The defining equations of the system can be put in the following form.

Buck converter:

$$L\frac{dI}{dt} = V_g u - V_0; \tag{1}$$

$$C\frac{dV_0}{dt} = I - \frac{V_0}{R}. \tag{2}$$

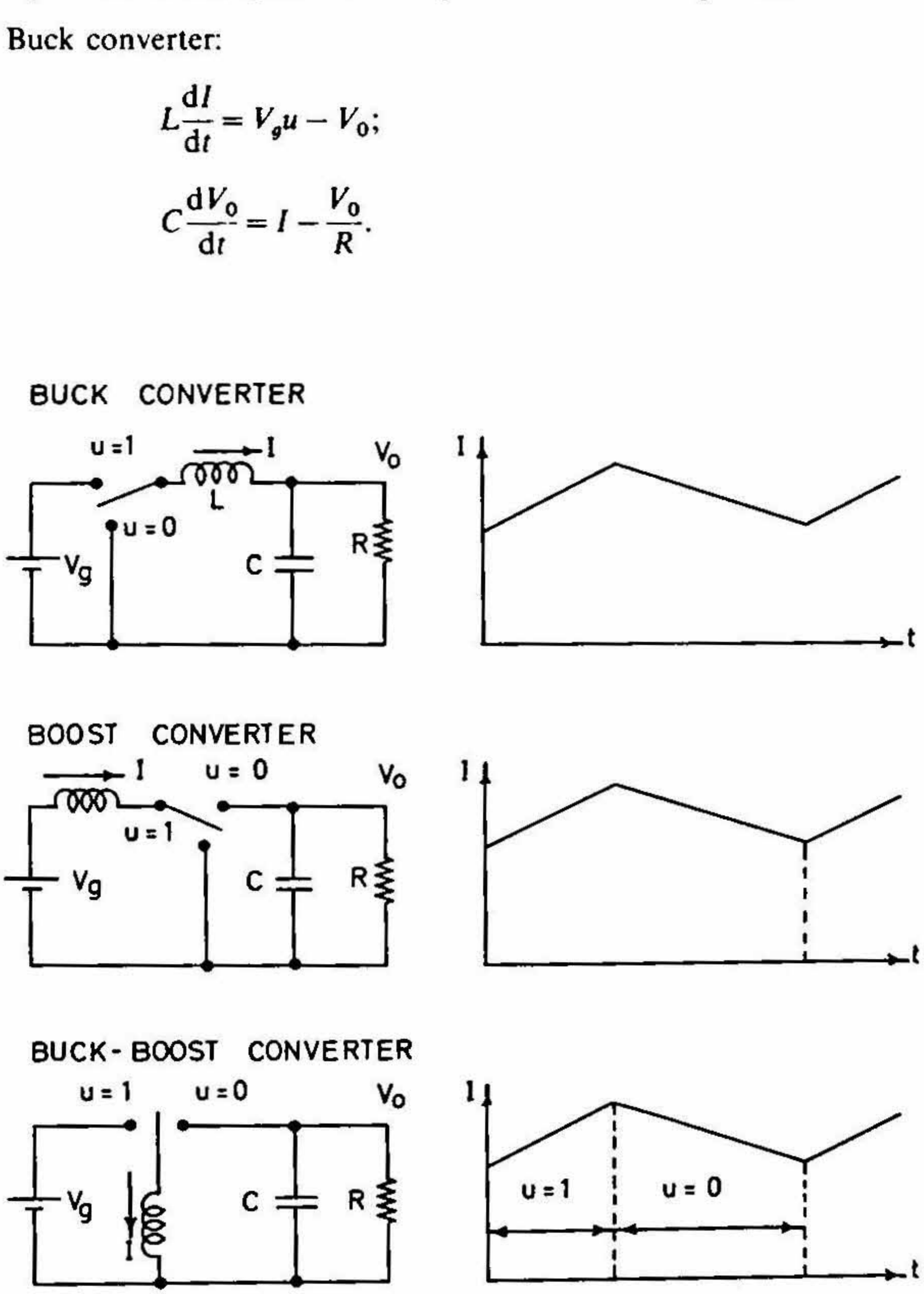

FIG. 1. The three basic switching converter topologies and their inductor current waveforms. The control input u as a function of the switch position is defined.

Boost converter:

$$L\frac{dI}{dt} = V_g - V_0\bar{u}; \tag{3}$$

$$C\frac{dV_0}{dt} = I\bar{u} - \frac{V_0}{R}. \tag{4}$$

Buck-boost converter:

$$L\frac{dI}{dt} = V_g u + V_0\bar{u}; \tag{5}$$

$$C\frac{dV_0}{dt} = -I\bar{u} - \frac{V_0}{R} \tag{6}$$

where $\bar{u} = 1 - u$. The systems are time variant and discontinuous, but the time variance and the discontinuities have been isolated into the single control-input variable u.

The description of all the above converters may be expressed in the following compact form.

$$\dot{X} = AX + Bu + T \tag{7}$$

where, for

Buck converter:

$$X = \begin{bmatrix} I \\ V_0 \end{bmatrix}; \quad A = \begin{bmatrix} 0 & -1/L \\ 1/C & -1/RC \end{bmatrix}; \quad B = \begin{bmatrix} V_g/L \\ 0 \end{bmatrix}; \quad T = \begin{bmatrix} 0 \\ 0 \end{bmatrix}.$$

Boost converter:

$$X = \begin{bmatrix} I \\ V_0 \end{bmatrix}; \quad A = \begin{bmatrix} 0 & -1/L \\ 1/C & -1/RC \end{bmatrix}; \quad B = \begin{bmatrix} V_0/L \\ -I/C \end{bmatrix}; \quad T = \begin{bmatrix} V_g/L \\ 0 \end{bmatrix}.$$

Buck-boost converter:

$$X = \begin{bmatrix} I \\ V_0 \end{bmatrix}; \quad A = \begin{bmatrix} 0 & +1/L \\ -1/C & -1/RC \end{bmatrix}; \quad B = \begin{bmatrix} (V_g - V_0)/L \\ I/C \end{bmatrix}; \quad T = \begin{bmatrix} 0 \\ 0 \end{bmatrix}.$$

The system state vector X and the matrices A, B and T are all continuous. Our ultimate objective is to synthesize the discontinuous control u in order to achieve the performance specification of the converter. First we briefly explain the method of sliding-mode control in general, before introducing the concept of equivalent control.

3. Sliding-mode control

Consider the single-input-single-output system represented in the controllable canonical form:

$$\dot{Y} = A^*Y + B^*u + T^* \qquad Y = \left[y_0 \frac{dy_0}{dt} \cdots \frac{d^{n-1}y_0}{dt^{n-1}} \right]^T \qquad u \in \{0, 1\} \tag{8}$$

where A^*, B^*, and T^* are system matrices and Y represents the system state errors. Equation (8) differs from eqn (7) since the states of the system are reassigned to be the output error and its successive derivatives, and the system matrices have been modified accordingly. Since Y represents the state errors, the desired operating point corresponds to $Y = 0$.

Suppose that the system states in the controllable canonical form (output y_0 and its successive derivatives) are all continuous, and accessible for measurement. The steady-state and dynamic requirements of the control problem such as steady-state error, overshoot, and settling time may be expressed in a single differential equation as follows.

$$g_0 y_0 + g_1 \frac{dy_0}{dt} + \cdots + g_{n-1} \frac{d^{n-1} y_0}{dt^{n-1}} = 0. \tag{9}$$

(For example, for a single-output second-order system we may indicate zero steady-state error, no overshoot, and settling time within 3τ as $y_0 + \tau\, dy_0/dt = 0$.)

For convenience, eqn (9) may be rewritten in the following form.

$$\sigma = GY = g_0 y_0 + g_1 \frac{dy_0}{dt} + \cdots + g_{n-1} \frac{d^{n-1} y_0}{dt^{n-1}} = 0 \tag{10}$$

where $G = [g_0 g_1 \cdots g_{n-1}]$. The output error y_0 and its successive derivatives are the states of the system, and the coefficients g_0 etc., may be thought of as the feedback gains for the different states of the system that are fed back. The quantity σ as expressed in eqn (10) is the weighted sum of the states of the system.

For the ideas that are being put forth below it is helpful to visualise eqn (10) geometrically as an $n-1$ dimensional surface in the n-dimensional space whose axes are the different states of the system. The principle of sliding-mode control is to forcibly constrain the system, by suitable control strategy, to stay on the sliding surface denoted by eqn (10). It may be pointed out here that though the terminology 'sliding surface' is an accepted one in the literature of sliding-mode control, one must remember that sliding surface is the surface on which the operating point slides; the surface itself does not slide.

When the system is constrained by sliding control to operate on the sliding surface described by eqn (10), it follows that the system dynamics are dictated by eqn (9). To force the system states to satisfy $\sigma = 0$, one must ensure that the system is capable of reaching the state $\sigma = 0$ from any initial condition and, having reached $\sigma = 0$, that the control is capable of maintaining the system at $\sigma = 0$. These conditions may be mathematically expressed as[1]:

$$\lim_{\sigma > 0} \dot{\sigma} < 0 \quad \text{and} \quad \lim_{\sigma < 0} \dot{\sigma} > 0. \tag{11}$$

It is worthwhile to express the above equation in words. When the system state is away from the surface denoted by $\sigma = 0$, the motion of the system state with respect to time ($d\sigma/dt$) is in such a direction as to move towards the surface $\sigma = 0$. Therefore to achieve the dynamic requirements given by eqn (9), the discontinuous control input u must be chosen such that eqn (11) is satisfied. Let

$$u = \begin{cases} u^+ & \text{for } \sigma > 0 \\ u^- & \text{for } \sigma < 0 \end{cases} \tag{12}$$

From eqns (8), (10), and (12)

$$\dot{\sigma} = \begin{matrix} GA^*Y + GB^*u^+ + GT^* & \text{for } \sigma > 0 \\ GA^*Y + GB^*u^- + GT^* & \text{for } \sigma < 0 \end{matrix} \tag{13}$$

Substitution from eqn (11) into eqn (13), leads to

$$GA^*Y + GB^*u^+ + GT^* < 0 < GA^*Y + GB^*u^- + GT^*. \tag{14}$$

Implementation of the control decision given by eqn (11) involves measurement of $\sigma = GY$ which is a weighted sum of the states of the system. Therefore it is necessary that all the controllable states of the system be continuous and accessible. Once eqns (10) and (11) are satisfied, the system dynamics are solely determined by the sliding surface (in turn by the elements of G) and are independent of the parameters of the system[1].

4. Equivalent control

Although the control variable u is a discontinuous function, one may obtain, as far as the low-frequency dynamics are concerned, under sliding motion, an equivalent system description where the discontinuous control u is replaced by an equivalent continuous control u_{eq}^1, as described below.

When sliding mode exists,

$$\sigma = \dot{\sigma} = 0. \tag{15}$$

From eqns (8) and (15), under sliding control

$$u_{eq} = -(GB^*)^{-1}[GA^*Y + GT^*]. \tag{16}$$

The system description now reduces to

$$\dot{Y} = [I - B^*(GB^*)^{-1}G](A^*Y + T^*). \tag{17}$$

Under ideal sliding-mode control, the switching frequency is infinite and eqn (17) is always valid. In real sliding-mode control, the sliding surface expands to a finite volume, around the ideal sliding surface, determined by the hysteresis of the switching action. The switching frequency is then finite and the validity of eqn (17) is restricted to a fraction of the switching frequency. When $\sigma \neq 0$, eqn (16) has the form

$$u_{eq} = -(GB^*)^{-1}[GA^*Y + GT^*] + (GB^*)^{-1}\dot{\sigma} \tag{18}$$

where u_{eq} is the equivalent control input for the system motion along a non-stationary sliding surface. The system dynamics are then given by

$$\dot{Y} = [I - B^*(GB^*)^{-1}G](AY^* + T^*) + B^*(GB^*)^{-1}\dot{\sigma}. \tag{19}$$

The first two terms of eqn (19) give the average motion of the system and the last term, the inter-cycle motion.

5. Duty ratio-controlled dc-to-dc converters

The equivalent control method is now illustrated to develop the system description of duty ratio-controlled dc-to-dc converters. Figure 2 shows the block diagram of constant

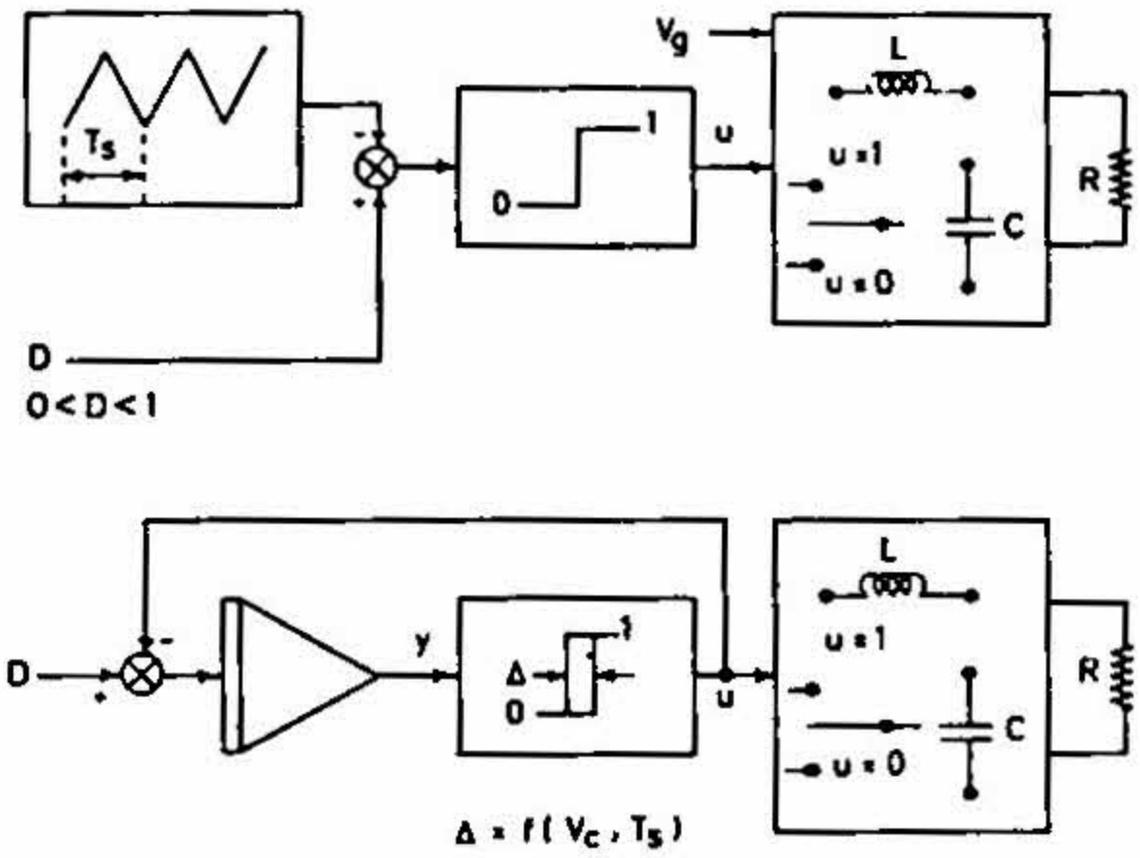

FIG. 2. Duty-ratio-controlled dc-to-dc converters and their equivalent representation. The ramp generator defining the switching frequency is incorporated as an integrator to enable mathematical representation of the system.

frequency duty ratio-controlled dc-to-dc converters. From the equivalent system of such converters also shown in fig. 2, one may write the following equations.

$$\dot{y} = D - u \tag{20}$$

$$\dot{X} = AX + Bu + T \tag{21}$$

where D is the duty ratio. Equations (20) and (21) may be combined into a single system:

$$\begin{bmatrix} \dot{y} \\ \dot{X} \end{bmatrix} = \begin{bmatrix} 0 & 0 \\ 0 & A \end{bmatrix} \begin{bmatrix} y \\ X \end{bmatrix} + \begin{bmatrix} -1 \\ B \end{bmatrix} u + \begin{bmatrix} D \\ T \end{bmatrix}. \tag{22}$$

In general, for a system of order n with m control inputs the sliding surface is of dimension $n-m$. In the present example, the system order is 3 and the number of control inputs is 1. The sliding surface in this case is a plane in the state-space given by $y=0$. The control input is

$$u = \begin{matrix} 1 & \text{for } \sigma = y > 0 \\ 0 & \text{for } \sigma = y < 0 \end{matrix}. \tag{23}$$

Under sliding control $\sigma = \dot{\sigma} = 0$, which leads to $u_{eq} = D$. The equivalent system description then becomes

$$\dot{X} = AX + BD + T. \tag{24}$$

Equation (24) is in general nonlinear. We have not invoked any constraints on the validity of eqn (24) other than the existence of sliding-mode control ($\sigma = 0$). Equation (24) can therefore be used to study both large- and small-signal performance. Or one can linearise the system around the operating point and obtain the small-signal transfer functions between the system states and the duty ratio, leading to the same results one would obtain following the state-space averaging method[3].

6. Buck converter in the phase plane

For a simple second-order system such as the buck converter, the simplicity of sliding-mode control is strikingly brought out by the phase-plane description of the system and the state trajectories for the switching inputs available for the system.

Figure 3 shows the phase-plane of the buck converter. The system states are the output-voltage error and the derivative of the output voltage (*i.e.* the capacitor current to some scale). The instantaneous state of the system is represented on the phase-plane by a point given by the output voltage error and the derivative of the output voltage at that instant. If the system state is known at any instant, the switch position at that instant along with the input voltage uniquely determines the future evolution of the system states for the duration of the switch in that position.

The system order being 2 and the number of control inputs being 1, the sliding surface is in this case a sliding line (one-dimensional surface). The sliding line shown in fig. 3 as $\sigma = 0$ partitions the phase-plane into two regions ($\sigma < 0$ and $\sigma > 0$). The significance of the special shape of the sliding line is explained later. The control input, namely, the switch position, is also shown in fig. 3 corresponding to the state of the converter. The steady-state operating point for each control input may be seen to be located in the opposite region. As a result, any switching action causes the system state to move towards the sliding line and cross into the other region. When the switching law as shown in fig. 3 is implemented, the system state moves towards the sliding line and having hit the sliding line, slides along the line to the final steady state, namely, the origin.

Since the system motion is constrained to be on the sliding line at all times, the response depends only on the chosen sliding line and is independent of the system parameters.

It may be noted that the sliding line is shaped such that the system states are constrained to be limited along the vertical axis. Such a limit conveniently provides overcurrent protection of the switch since the vertical axis also represents the capacitor current to some scale and in turn the current through the switch.

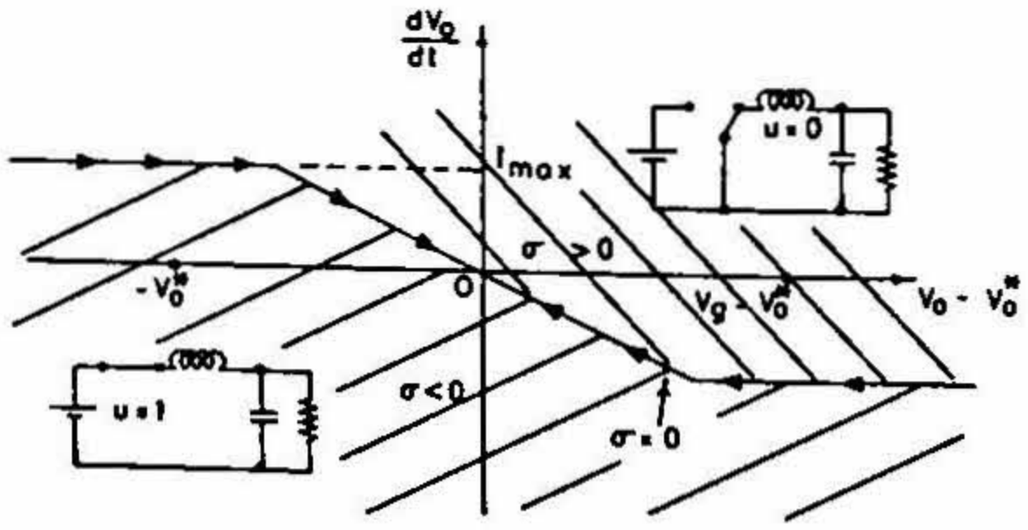

FIG. 3. The phase-plane description of the buck converter. The sliding line $\sigma = 0$ partitions the phase-plane into two regions. The steady-state operating point for each of the converter topologies ($u = 1$ and $u = 0$) is seen to be located in the opposite region ($V_g - V_0^*$ and $-V_0^*$), respectively.

Figure 4 shows a typical starting transient in the phase-plane. Figure 5 shows the entire controller design process at one glance. Figure 6 shows typical response of a buck converter in the phase-plane to a step change in reference.

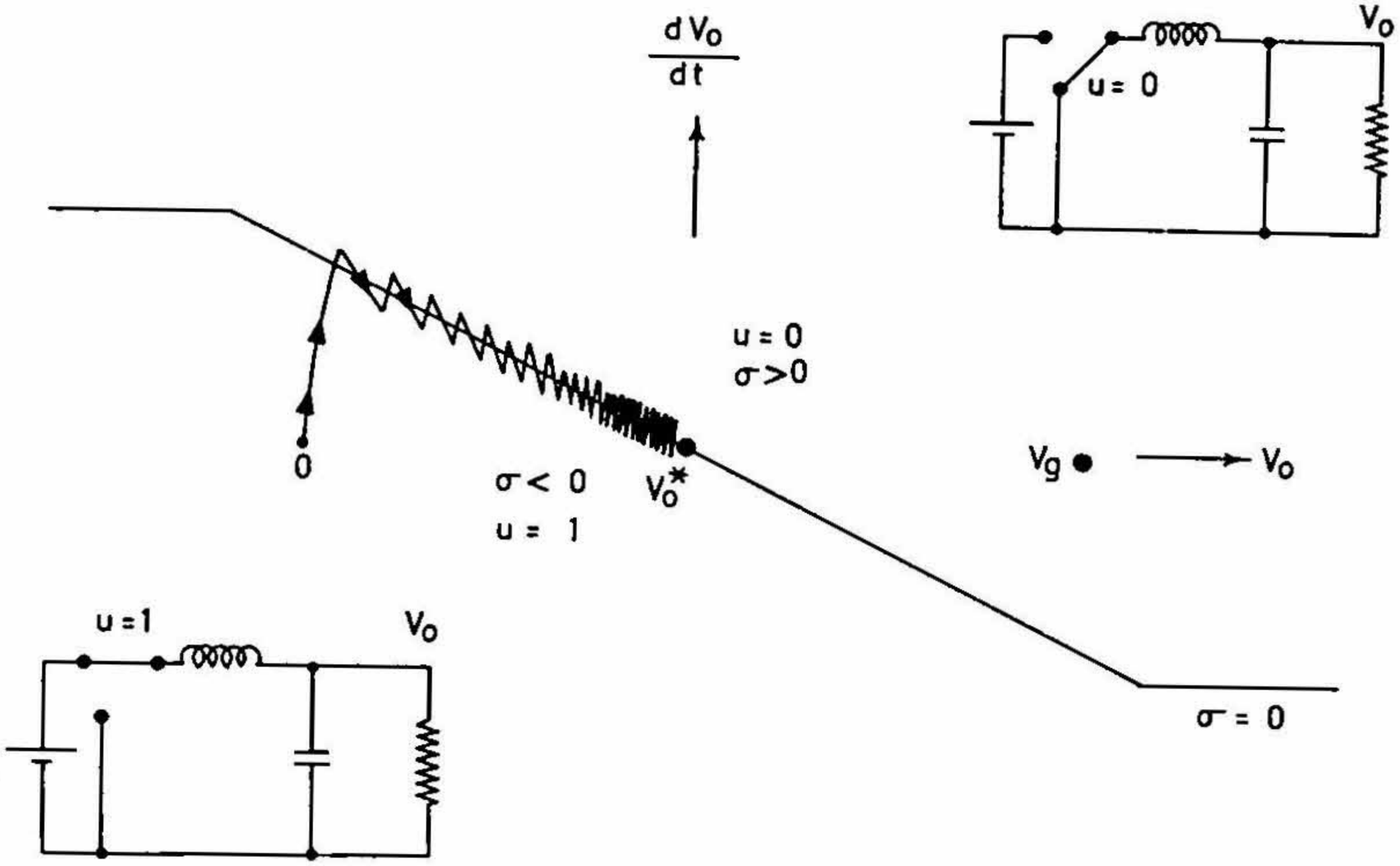

FIG. 4. The starting transient of a sliding-mode-controlled buck converter. The horizontal portions of the sliding line $\sigma=0$ indicate constant current operation. The middle region of the sliding line passing through the origin shows the voltage-controlled operation.

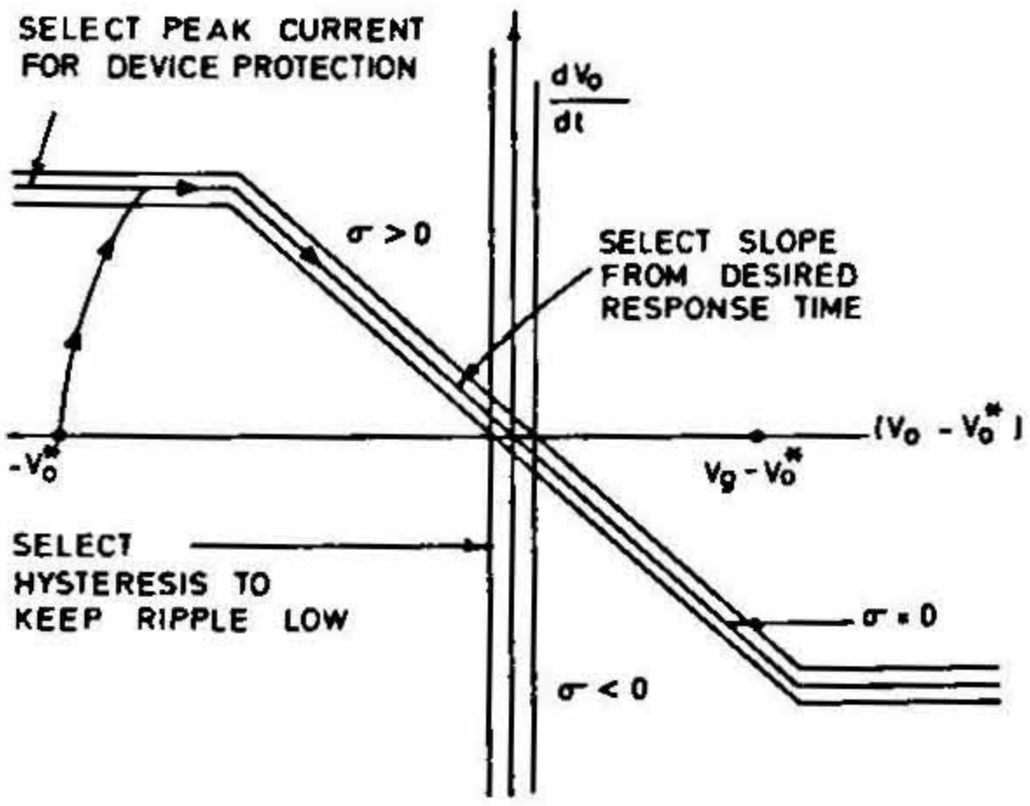

FIG. 5. Design process of a buck-converter controller. The current limit for the switch, the desired response time, and the nominal switching frequency are used to set up the desired sliding line.

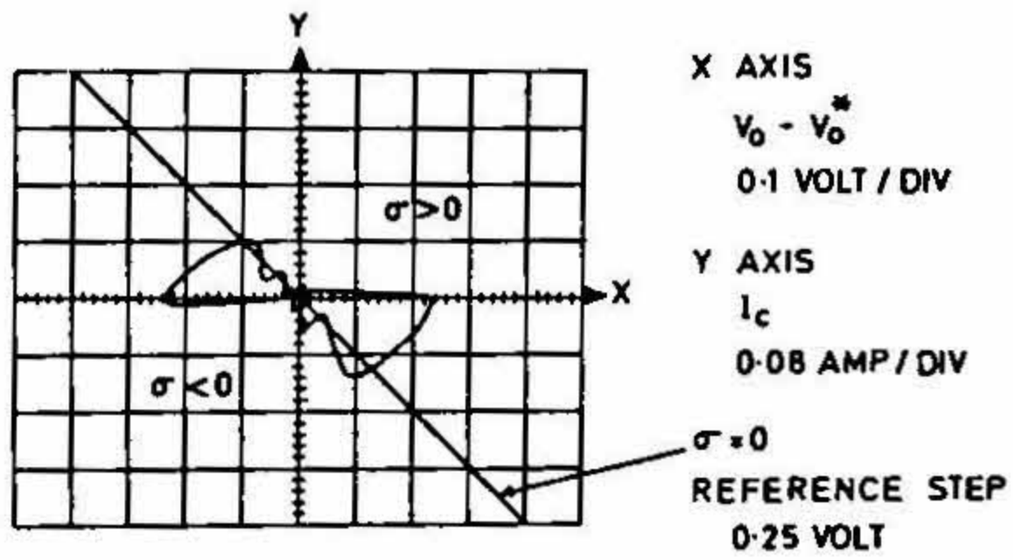

FIG. 6. Response to a reference step in the phase-plane for a buck converter. The steady-state operating point is the origin. Disturbances such as a step change in reference throw the system away from the origin. The recovery shows a two-part transient – one, reaching the sliding line $\sigma=0$, and two, sliding along the sliding line to the final steady-state.

7. Current-programmed dc-to-dc converters

For boost and buck-boost converters the application of sliding-mode control for output voltage regulation is not straight forward. Figure 7 shows the typical waveforms for a boost converter. It may be noticed that the derivative of the output voltage (the capacitor current to some scale) is discontinuous, and in the presence of parasitic series resistance in the output capacitor, the output voltage is also discontinuous. As a result, the strategy of control has to be different from that of buck converter.

Under inductor current control, all three topologies of converters are of reduced order and are equally amenable to the application of sliding-mode control.

Figure 8 shows the phase-plane of the boost converter. For inductor control the system order is 1 and so the phase-plane is really a phase-line (the X axis). The system state is the inductor current error. The two possible switch states are also shown in fig. 8. The sliding surface is zero-dimensional and reduces to a sliding point. The sliding point partitions the phase-line into two regions ($\sigma < 0$ and $\sigma > 0$). The steady-state operating point of each of the switch inputs is located in the opposite region thus satisfying the condition of sliding-mode control. It can be seen that the same is also true for the buck converter and the buck-boost converter.

We may apply the equivalent control method to arrive at small-signal models for the current-programmed converters. For the boost converter,

$$L\frac{\mathrm{d}I}{\mathrm{d}t} = V_g - V_0\bar{u}, \tag{25}$$

$$C\frac{\mathrm{d}V_0}{\mathrm{d}t} = I\bar{u} - \frac{V_0}{R}, \tag{26}$$

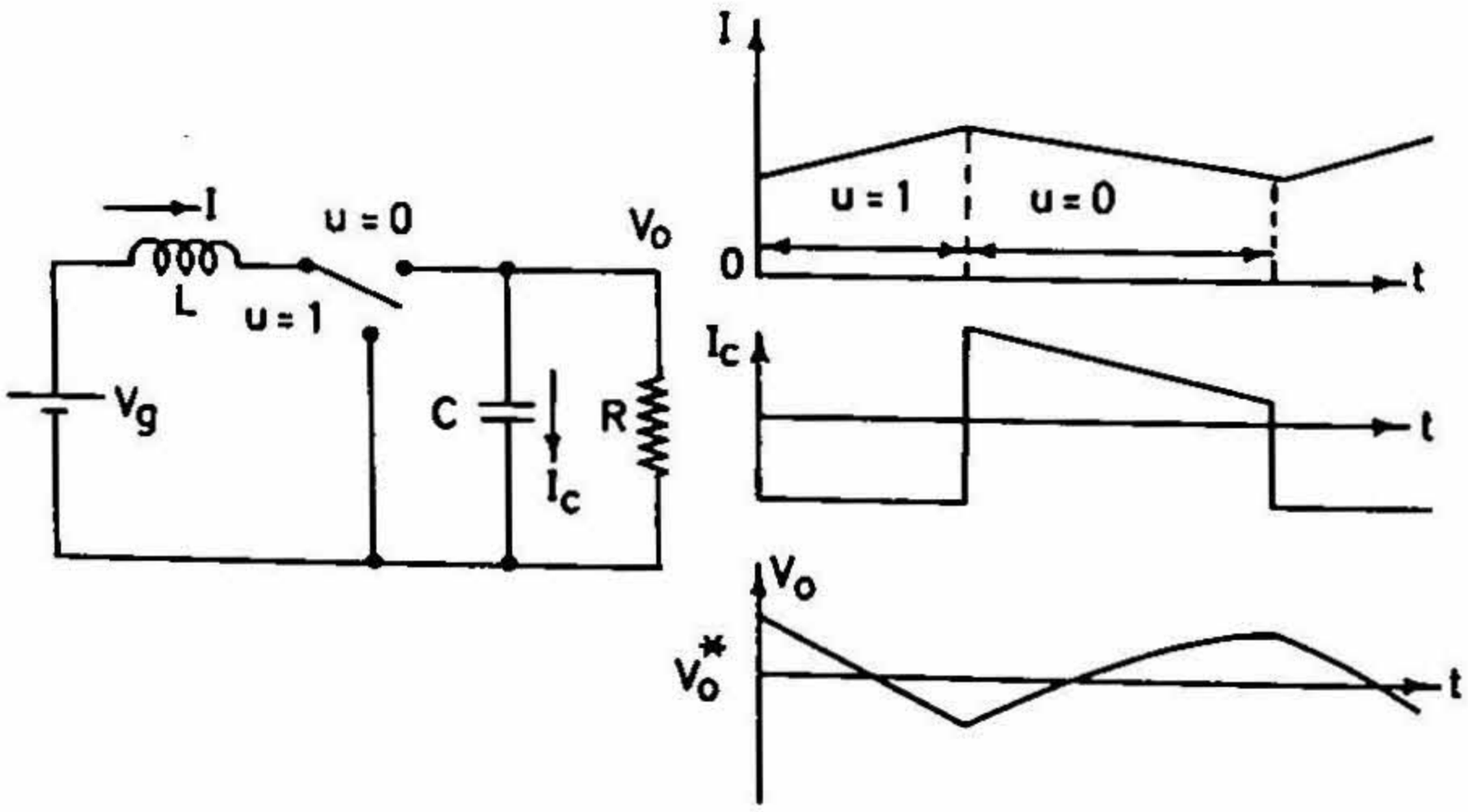

FIG. 7. Boost-converter topology and waveforms (output RC time constant is much higher than the switching frequency). The capacitor current, which is the same as the derivative of the output voltage to some scale, shows discontinuities at switching instants.

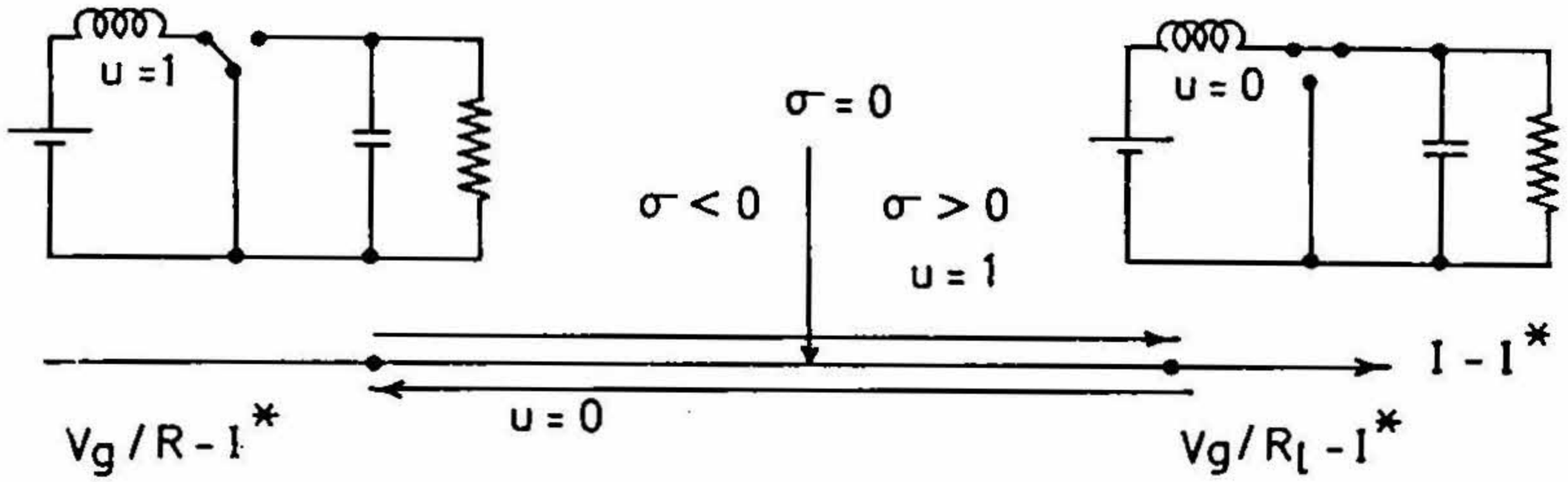

FIG. 8. Phase-line description of current-controlled boost converter. The sliding point $\sigma=0$ partitions the phase-line into two regions. The control input for each of the regions and the respective evolution of inductor currents are shown. R_1 is the resistance of the inductor winding.

$$\sigma = I - I^* \tag{27}$$

$$\bar{u}_{eq} = V_g / V_0. \tag{28}$$

Insertion of u_{eq} into eqn (26) leads to

$$V_g I = V_0^2/R + \mathrm{d}(CV_0^2/2)/\mathrm{d}t. \tag{29}$$

Under current-programmed control it is seen that the system is linear between the reference current and the square of the output voltage. One has to view this statement with caution, since this is true only when the system stays on the sliding point. When the system is not on the sliding point, as during the transients, $\mathrm{d}I/\mathrm{d}t$ is not zero and some error creeps in, which may be accounted as follows:

$$\bar{u}_{eq} = (V_g - L\mathrm{d}I/\mathrm{d}t)/V_0. \tag{30}$$

Insertion into eqn (26) and rearrangement leads to

$$V_g I = V_0^2/R + \mathrm{d}(CV_0^2/2)/\mathrm{d}t + \mathrm{d}(LI^2/2)/\mathrm{d}t. \tag{31}$$

Equation (31) is an illustrative description of any switching converter, and may be simply stated as

$$\begin{matrix}\text{Input} \\ \text{power}\end{matrix} = \begin{matrix}\text{Output} \\ \text{power}\end{matrix} + \begin{matrix}\text{Rate of change of} \\ \text{stored energy.}\end{matrix} \tag{32}$$

Equation (32) is valid for any system. It is especially valuable for the boost converter since in this case all the terms involved are continuous functions. Equation (32) is in general nonlinear between inductor current and output voltage, and is given below for different converters.

Buck converter:

$$V_g I u = V_0^2/R + \mathrm{d}(CV_0^2/2)/\mathrm{d}t + \mathrm{d}(LI^2/2)/\mathrm{d}t. \tag{33}$$

Boost converter:

$$V_g I = V_0^2/R + \mathrm{d}(CV_0^2/2)/\mathrm{d}t + \mathrm{d}(LI^2/2)/\mathrm{d}t. \tag{34}$$

Buck-boost converter:

$$V_g Iu = V_0^2/R + \mathrm{d}(CV_0^2/2)/\mathrm{d}t + \mathrm{d}(LI^2/2)/\mathrm{d}t. \tag{35}$$

The above equations may be perturbed as

$$I = I^* + \hat{I}; \quad V_0 = V_0^* + \hat{V}_0$$

and linearised around the operating point to get the small-signal transfer function between control current and output voltage.

Buck converter:

$$\frac{\hat{V}_0(S)}{\hat{I}(S)} = \frac{R}{1 + SCR}. \tag{36}$$

Boost converter:

$$\frac{\hat{V}_0(S)}{\hat{I}(S)} = \frac{RV_g}{2V_0^*} \frac{1 - SLV_0^{*2}/RV_g^2}{1 + SCR/2}. \tag{37}$$

Buck-boost converter:

$$\frac{\hat{V}_0(S)}{\hat{I}(S)} = -\frac{RV_g}{V_g - 2V_0^*} \frac{1 - SLV_0^*(V_g - V_0^*)/RV_g^2}{1 + SCR(V_g - V_0^*)/(V_g - 2V_0^*)}. \tag{38}$$

Middlebrook and Cuk[4] arrived at the same results by the state-space averaging method.

8. Sliding-mode voltage control

It was observed that, under output-voltage regulation, the boost and buck-boost converters exhibit discontinuities in their controllable states. As a result, the simple approach suitable for the control of buck converter is not applicable for the voltage control of boost and buck-boost converters. One approach is to establish an inner loop as a sliding-mode current controller and then to implement an outer voltage-control loop based on the small-signal linear model of the current-controlled converters. The linear models established in eqns (37) and (38) may be used for this approach.

An alternative approach is to implement a direct sliding-mode voltage regulator. After all, the state assignment to a system is not unique, and therefore we may try setting up the sliding surface in terms of as many identifiable continuous states of the system as the order of the system, and then relate the resultant dynamics to the desired response.

8.1. *Inductor current to output voltage transformation*

The inductor current I and the output voltage V_0 (in the absence of equivalent series resistance of the capacitor) are continuous variables and qualify as suitable states in terms of which the sliding surface may be set up. In order to study the stability of the trajectories on such a sliding surface, one has to transform the sliding surface in terms of output voltage and its derivatives. The equivalent system description given by eqns (33) to (35) may be

used to obtain this transformation between the inductor current and output voltage. The method is illustrated for boost converter and the results are presented for the other converters.

For boost converter, eqn (34) may be manipulated and rewritten as

$$V_0^2 + RCV_0\,\mathrm{d}V_0/\mathrm{d}t = RI(V_g - L\,\mathrm{d}I/\mathrm{d}t). \tag{39}$$

In practical converters, in order to obtain good small-signal response as well as large power bandwidth, it is necessary to choose L such that $V_g \gg L\,\mathrm{d}I/\mathrm{d}t$. Then eqn (39) reduces to

$$I = \frac{CV_0}{V_g}\frac{\mathrm{d}V_0}{\mathrm{d}t} + \frac{V_0^2}{RV_g}. \tag{40}$$

Equation (40) gives the relationship between inductor current and output voltage for the boost converter. This relationship is in general nonlinear and is given below for all the converters.

Buck converter:

$$I = C\frac{\mathrm{d}V_0}{\mathrm{d}t} + \frac{V_0}{R}. \tag{41}$$

Boost converter:

$$I = C\frac{V_0}{V_g}\frac{\mathrm{d}V_0}{\mathrm{d}t} + \frac{V_0^2}{RV_g} \qquad (V_g \gg L\,\mathrm{d}I/\mathrm{d}t). \tag{42}$$

Buck-boost converter:

$$I = \frac{C(V_d - V_0)}{V_g}\frac{\mathrm{d}V_0}{\mathrm{d}t} + \frac{V_g - V_0}{V_g}\frac{V_0}{R} \qquad (V_0 \gg L\,\mathrm{d}I/\mathrm{d}t). \tag{43}$$

In the next subsection sliding-mode control of boost converter is set up in terms of inductor current and output voltage. The relationship between inductor current and output voltage given by eqn (42) is then used to analyse the stability of the sliding regime. The same method is applicable to all three dc-to-dc converters.

8.2. *Voltage control of boost converter*

For boost converter, from eqn (42), it is seen that the inductor current contains the voltage-derivative information. The boost converter being a second-order system, the gain matrix G is a 2×1 matrix and the sliding surface may be set up as

$$\sigma = GY = K_v(\hat{v}_0 + R_s\hat{i}) \tag{44}$$

where $\hat{v}_0$ and $\hat{i}$ represent the voltage and current errors, respectively.

Comparing eqn (44) with the general sliding surface given by eqn (10) one may identify the feedback-gain parameters g_0 as K_v and g_1 as K_vR_s. Let us identify the practical significance of the different gain parameters. The parameter R_s is in practice the current-sensing resistance. It is good to remember that in practice the current-sensing

resistance is usually orders of magnitude less than the load resistance, R. Under sliding-mode control, $\sigma=0$ and so K_v does not influence the response. It is significant only as a scale factor of the sliding surface. In ideal sliding-mode control, switching takes place in an infinitismal vicinity around $\sigma=0$, and so K_v has no significance whatsoever. However, in a real sliding-mode control, switching takes place in a finite vicinity around the sliding surface $\sigma=0$, and K_v then determines the nominal switching frequency for a given output ripple and *vice versa*.

We now go on to examine whether the trajectories along the sliding line lead to unique steady-state operating point. Define the current and voltage errors by the following relationship:

$$I = I^* + \hat{i} \tag{45}$$

$$V_0 = V_0^* + \hat{v}_0. \tag{46}$$

Equation (42) gives the relationship between inductor current and output voltage for boost converter. This relationship may be written in terms of voltage and current errors as follows.

$$I^* + \hat{i} = C\frac{V_0^* + \hat{v}_0}{V_g}\frac{\mathrm{d}(V_0^* + \hat{v}_0)}{\mathrm{d}t} + \frac{(V_0^* + \hat{v}_0)^2}{RV_g}. \tag{47}$$

Separating the dc and ac quantities, we get

$$I^* = V_0^{*2}/RV_g, \tag{48}$$

$$\hat{i} = \frac{CV_0^*}{V_g}\frac{\mathrm{d}\hat{v}_0}{\mathrm{d}t} + \frac{2V_0^*}{RV_g}\hat{v}_0 + \frac{C}{2V_g}\frac{\mathrm{d}(\hat{v}_0)^2}{\mathrm{d}t} + \frac{\hat{v}_0^2}{RV_g}. \tag{49}$$

Using eqn (49), we may transform the sliding surface eqn (44) as follows.

$$\sigma = K_v\left[\hat{v}_0 + \frac{2V_0^*R_s}{RV_g}\hat{v}_0 + \frac{CV_0^*R_S}{V_g}\frac{\mathrm{d}\hat{v}_0}{\mathrm{d}t} + \frac{R_S\hat{v}_0^2}{RV_g} + \frac{CR_S}{2V_g}\frac{\mathrm{d}(\hat{v})_0^2}{\mathrm{d}t}\right]. \tag{50}$$

Equation (50) may be rearranged and written as

$$\sigma = K_v[a(t)\hat{v}_0 + b(t)\,\mathrm{d}\hat{v}_0/\mathrm{d}t] \tag{51}$$

where

$$a(t) = 1 + \frac{R_SV_0^*}{RV_g}[2 + \hat{v}_0/V_0^*] \tag{52}$$

$$b(t) = \frac{CR_SV_0^*}{V_g}[1 + \hat{v}_0/V_0^*]. \tag{53}$$

It is to be noted that we have not yet invoked any restriction on the validity of eqn (51), small signal or otherwise. Equation (50) is a first-order differential equation. The condition for guaranteed stability of response along the sliding line turns out to be that both $a(t)$ and $b(t)$ be positive. Or a sufficient condition in terms of the alternating quantity $\hat{v}_0$ is that the relative error $\hat{v}_0/V_0^*$ be less than 1.

Alternatively eqn (51) may be interpreted differently as follows. For large errors the $\hat{v}_0^2$ terms dominate, and so the sliding line is determined mainly by terms containing $\hat{v}_0^2$; for

small errors, the $\hat{v}_0$ terms dominate. The response can therefore be thought of as having two parts.

Large-signal response:

$$\hat{v}_0^2 + \frac{RC}{2}\frac{d\hat{v}_0^2}{dt} = 0. \tag{54}$$

Small-signal response:

$$\hat{v}_0 + \frac{2V_0^* R_S}{RV_g}\hat{v}_0 + \frac{CV_0^* R_S}{V_g}\frac{d\hat{v}_0}{dt} = 0. \tag{55}$$

The large-signal response is truly a constant current response that is stable and with a time constant determined by the output circuit elements (RC/2). The small-signal response is decided by the feedback gain (the current-sensing resistance, R_s) and the operating point. The important point to notice is that the system is always stable for large signals. The small-signal stability is determined by the feedback gain.

The phase-plane representation of the boost converter is shown in fig. 9. The axes are the inductor current and the output voltage. The operating point under sliding-mode control has to satisfy two conditions, namely $\sigma = 0$ and the steady-state gain of $I^* = V_0^{*2}/RV_g$. Curve I in the phase-plane represents the dc gain. Line II is the sliding line $\sigma = 0$. The

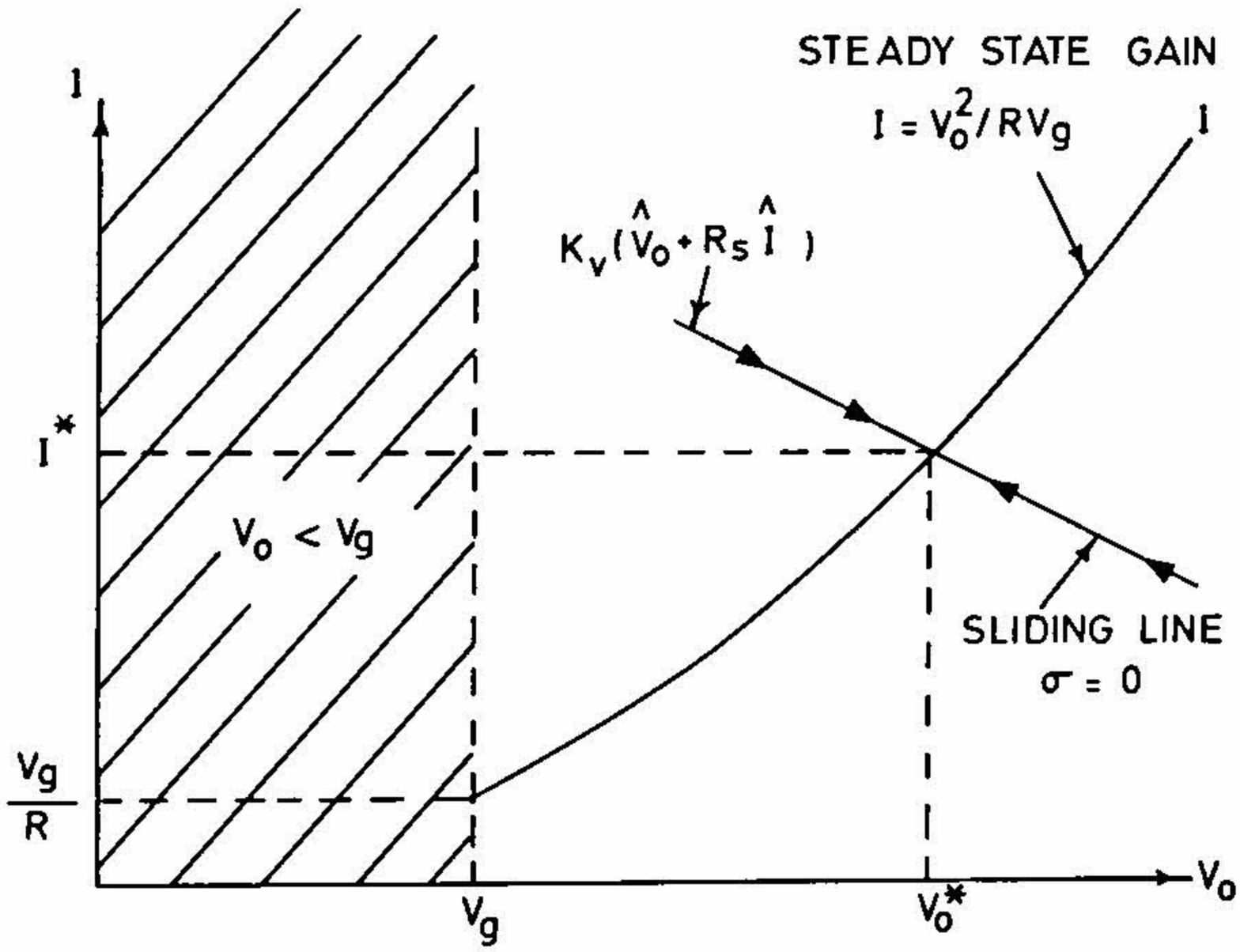

FIG. 9. The phase-plane of the boost converter with the inductor current and the output voltage as the states of the converter. Line I shows the steady-state gain between inductor current I and output voltage V_0. $\sigma = 0$ is the proposed sliding line. Under sliding-mode control both the steady state and the sliding condition are satisfied, giving rise to the operating point (I^*, V_0^*).

sliding line is centred on the operating point with a slope of $-R_s$. The system state, if confined to move on the sliding line, eventually reaches the steady-state operating point (V_0^*, I^*).

9. Practical considerations

Since it is established that large-signal stability is always guaranteed, the design may be conveniently based on the small-signal model. From eqn (49), for small errors

$$\hat{i} = \frac{CV_0^*}{V_g}\frac{d\hat{v}_0}{dt} + \frac{2V_0^*}{RV_g}\hat{v}_0 \tag{56}$$

where $\hat{i}$ is defined as the current error. To measure $\hat{i}$, the average value I^* must be subtracted out of the total inductor current I. This is accomplished by the use of a high-pass filter in the inductor current measurement. The simplest form of filter function is a single inverted pole at w_1. Further, since eqn(10) for the sliding surface is a linear differential equation, we can express the sliding surface in the frequency domain as well. Let

$$\sigma(S) = K_v\left\{\hat{v}_0(S) + \frac{1}{1 + w_1/S}R_S\hat{i}(S)\right\}. \tag{57}$$

Equations (56) and (57) may be combined to obtain

$$\sigma(S) = K_v\frac{1 + \dfrac{2R_SV_0^*}{RV_g} + \dfrac{w_1}{S} + \dfrac{CR_SV_0^*}{V_g}S}{1 + \dfrac{w_1}{S}}\hat{v}_0(S) \tag{58}$$

$$\simeq K_v\frac{1 + \dfrac{w_1}{S} + \dfrac{S}{w_M}}{1 + \dfrac{w_1}{S}}\hat{v}_0(S) \tag{59}$$

in which the (good) approximation always obtains because the current-sensing resistance, R_s, is much smaller than the load resistance, R, and where

$$w_M = \frac{1}{CR_S}\frac{V_g}{V_0^*}. \tag{60}$$

In the ideal case in which the current error $\hat{i}$ could be measured without a filter, $w_1 = 0$ and eqn (59) reduces to

$$\sigma(S) = K_v\,(1 + S/w_M)\hat{v}_0(S) \tag{61}$$

or, in the time domain as

$$\sigma(t) = K_v\left\{\hat{v}_0(t) + \frac{1}{w_M}\frac{d\hat{v}_0(t)}{dt}\right\}. \tag{62}$$

Therefore, w_M is the maximum bandwidth that can be obtained or, in the time-domain, the fastest transient response of the output error is characterized by a time constant $1/w_M$ that depends on the system parameters (C, V_0, V_g) and the current-sensing resistance (R_s).

In the realistic case of a non-zero filter-corner frequency, w_1, eqn (59) may be factored so that

$$\sigma(S) = K_v \frac{(1 + w_1/S)(1 + S/w_M)}{(1 + w_1/S)} \hat{v}_0(S) \tag{63}$$

$$= K_v(1 + S/w_M)\hat{v}_0(S) \tag{64}$$

which is the same ideal result as eqn (61). Therefore the condition that the factorization be valid, which is $w_1 \ll w_M$, becomes a design criterion: to retain the maximum bandwidth response, it is necessary only that the filter corner be chosen much lower than the maximum bandwidth itself.

Figure 10 shows the schematic diagram of a sliding-mode controller for a boost converter. Figure 11 shows the response of the converter to step changes in reference and in

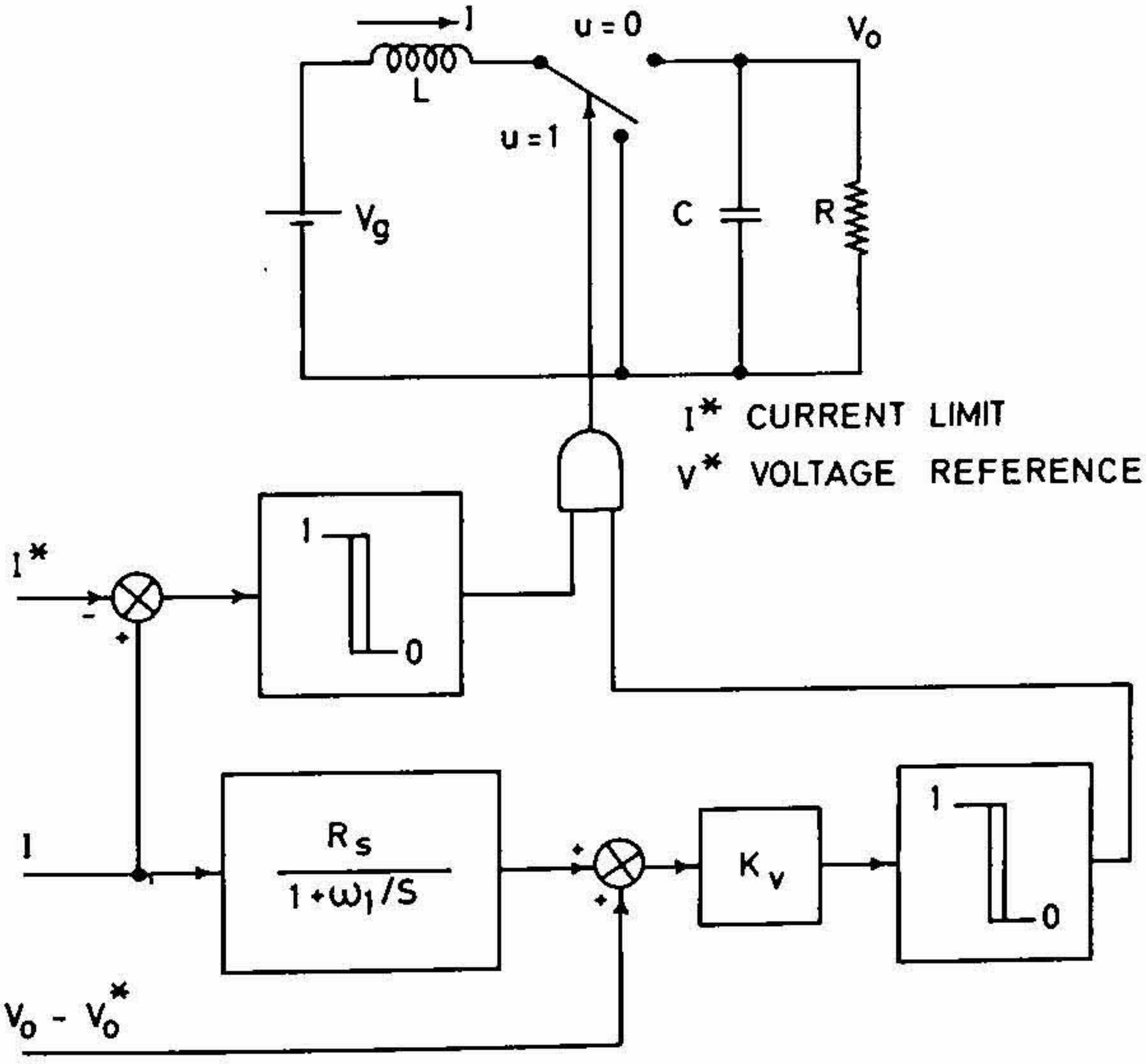

FIG. 10. Sliding-mode controller for the boost converter. The high-pass filter for current measurement effectively isolates the steady-state value of I. The current limit overrides the control when the inductor current exceeds a pre-set limit.

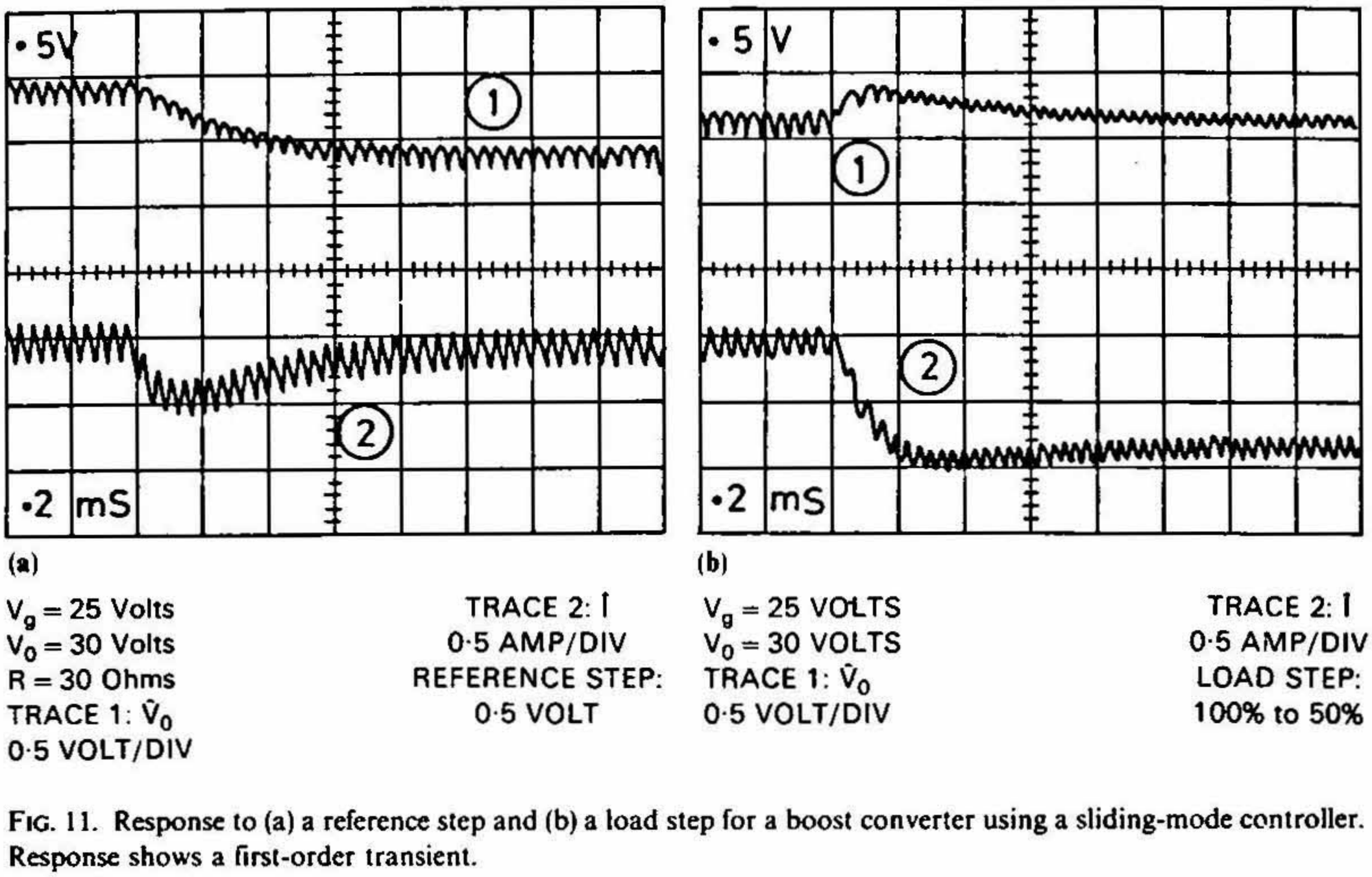

FIG. 11. Response to (a) a reference step and (b) a load step for a boost converter using a sliding-mode controller. Response shows a first-order transient.

load. It is seen in both the step responses the effective response is first order by virtue of the design criterion $w_1 \ll w_M$.

9.1. *Effect of ESR of output capacitor*

In a practical converter, the output capacitor is not ideal and will have a parasitic equivalent series resistance (ESR). The output voltage therefore will be discontinuous at the switching instants. Figure 12 shows the inductor current, output voltage, and the switching function $\sigma(t)$. The switching function σ is seen to have discontinuities. However this does not affect the performance of the sliding-mode controller other than decreasing the switching frequency. It will be helpful to use a low-pass filter for measuring the output voltage with a corner just above the switching frequency.

10. Conclusion

Sliding-mode control of a class of dc-to-dc converters is introduced in a formal manner. The same concept is presented in the case of buck converter through a more illuminating graphical way. The concept of equivalent control as an analytical tool is demonstrated for constant frequency duty-ratio-controlled converters. The simplicity of the control of current-programmed converters is brought out, and again the application of the equivalent control method is shown to lead to an alternative method of setting up the sliding line for the voltage control of boost and buck-boost converters. Stability of control is shown to be guaranteed

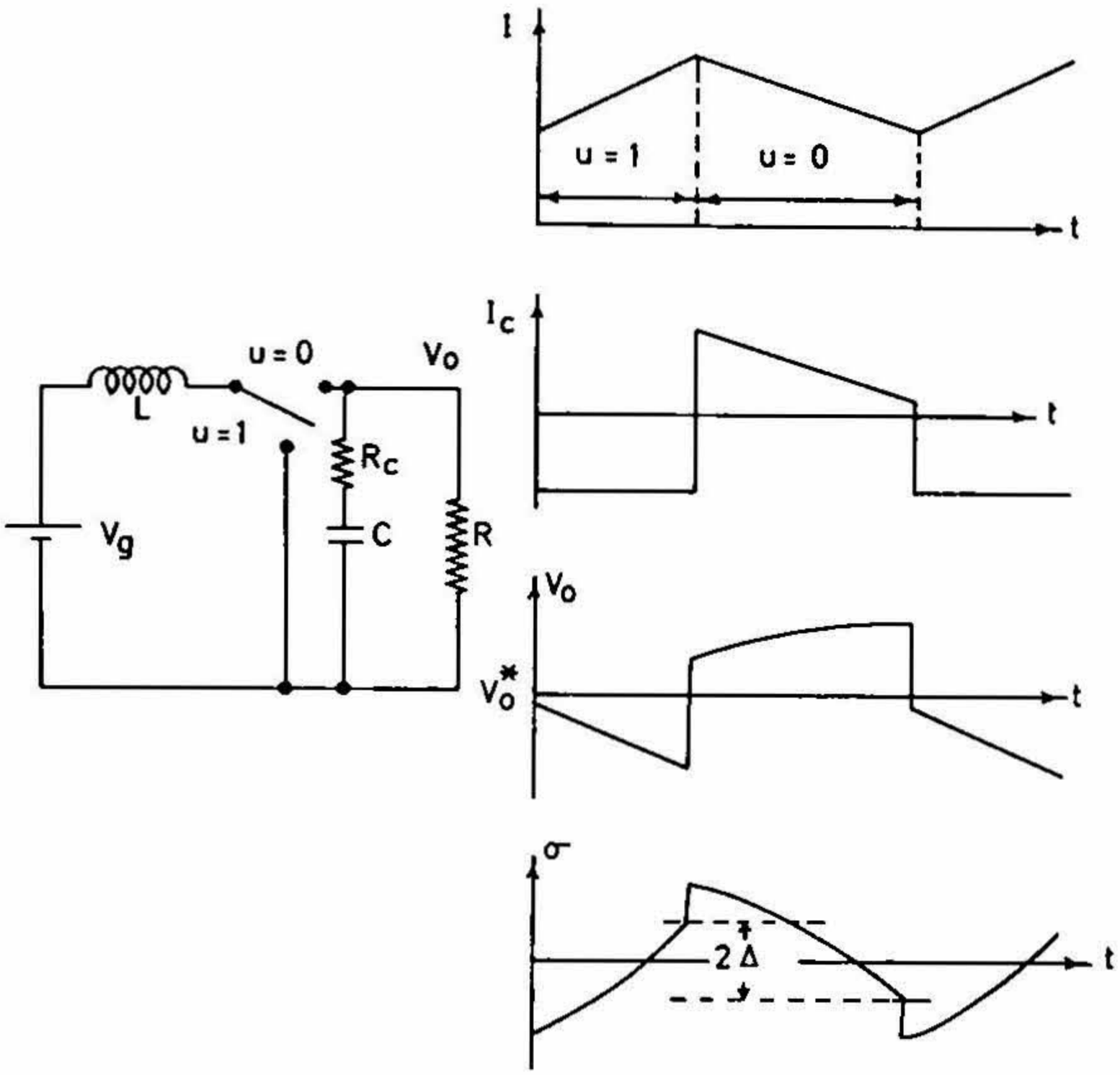

FIG. 12. The boost converter with the ESR of the output capacitor and the various steady-state waveforms. The switching function σ also exhibits discontinuities. This, however, does not affect the low-frequency performance of the converter. The switching frequency is seen to reduce owing to the effects of ESR.

for both small and large signals. Experimental results are shown to verify the control concepts.

References

1. UTKIN, V. I. *Sliding modes and their application in variable structure systems*, Mir, Moscow, 1978.

2. BILALOVIC, F., MUSIC, O. AND SABANOVIC, A. Buck converter regulator operating in the sliding mode, *Proc. Seventh Int. PCI'83 Conf.*, pp. 331–340, 1983.

3. MIDDLEBROOK, R. D. AND CUK, S. M. *Advances in switched mode power conversion*, Vols I & II, TESLAco, Pasadena, Second edn, 1983.

4. VENKATARAMANAN, R. *Sliding mode control of power converters.* Ph.D. Thesis, Caltech, Pasadena, 1986.